

2+1 flavor lattice QCD simulation with $O(a)$ -improved Wilson quarks

**PACS-CS Collaboration : N. Ukita^{*a†}, S. Aoki^{b,c}, N. Ishii^a, K.-I. Ishikawa^d,
N. Ishizuka^{a,b}, T. Izubuchi^{c,e}, D. Kadoh^a, K. Kanaya^b, Y. Kuramashi^{a,b}, Y. Namekawa^a,
M. Okawa^d, Y. Taniguchi^{a,b}, A. Ukawa^{a,b}, T. Yoshié^{a,b}**

^aCenter for Computational Sciences, University of Tsukuba, Tsukuba, Ibaraki 305-8577, Japan

^bGraduate School of Pure and Applied Sciences, University of Tsukuba, Tsukuba, Ibaraki 305-8571, Japan

^cRiken BNL Research Center, Brook-haven National Laboratory, Upton, New York 11973, USA

^dGraduate School of Sciences, Hiroshima University, Higashi-Hiroshima, Hiroshima 739-8526, Japan

^eInstitute for Theoretical Physics, Kanazawa University, Kanazawa, Ishikawa 920-1192, Japan

We present simulation details and results for the light hadron spectrum in $N_f = 2 + 1$ lattice QCD with the nonperturbatively $O(a)$ -improved Wilson quark action and the Iwasaki gauge action. Simulations are carried out at a lattice spacing of 0.09 fm on a $(2.9\text{fm})^3$ box using the PACS-CS computer. We employ the Lüscher's domain-decomposed HMC algorithm with several improvements to reduce the degenerate up-down quark mass toward the physical value. So far the resulting pseudoscalar meson mass is ranging from 702MeV down to 156MeV. We discuss on the stability and the efficiency of the algorithm. The light hadron spectrum extrapolated at the physical point is compared with the experimental values. We also present the values of the quark masses and the pseudoscalar meson decay constants.

The XXVI International Symposium on Lattice Field Theory
July 14-19 2008
Williamsburg, Virginia, USA

*Speaker.

†E-mail: ukita@ccs.tsukuba.ac.jp

1. Introduction

The PACS-CS (Parallel Array Computer System for Computational Sciences) project[1, 2, 3, 4, 5, 6, 7, 8] aims at $N_f = 2 + 1$ lattice QCD calculations at the physical point to remove the most troublesome systematic errors associated with the chiral extrapolations. So far our simulation points cover from 67MeV to 3.5MeV for the degenerate up-down quark mass with the strange quark mass fixed around the physical value. The reduction of m_{ud} down to 10 MeV is achieved by the domain-decomposed Hybrid Monte Carlo (DDHMC) algorithm with the replay trick[9, 10]. For the simulation at $m_{ud} = 3.5$ MeV we incorporate some algorithmic improvements such as the mass preconditioning[11, 12], the chronological inverter[13] and the deflation technique[14] which make simulations stable and contribute to reduce the simulation cost. For the strange quark part we employ the UV-filtered Polynomial Hybrid Monte Carlo (UVPHMC) algorithm[15].

In this report we present the simulation details and some eminent results for the hadron spectrum. Chiral analyses on the pseudoscalar meson sector with the SU(2) and SU(3) chiral perturbation theories and calculation of the charm quark systems with the relativistic heavy quark action are given in separate reports[16, 17].

2. Simulation details

We employ the $O(a)$ -improved Wilson quark action with a nonperturbative improvement coefficient $c_{sw} = 1.715$ [18] and the Iwasaki gauge action[19]. All the simulations are carried out on a $32^3 \times 64$ lattice at $\beta = 1.90$ corresponding to the lattice spacing of $a = 0.09$ fm. Table 1 summarizes our simulation parameters. We choose combinations of the hopping parameters (κ_{ud}, κ_s) based on the previous CP-PACS/JLQCD results[20, 21] except $(\kappa_{ud}, \kappa_s) = (0.137785, 0.13660)$ which is adjusted at the physical point with the use of the PACS-CS results in an early stage[8, 4]. The physics results at $(\kappa_{ud}, \kappa_s) = (0.137785, 0.13660)$ is presented in Ref. [7].

The DDHMC algorithm is implemented for the up-down quark by domain-decomposing the full lattice with an 8^4 block size as a preconditioner for HMC. The domain-decomposition factorizes the up-down quark determinant into the UV and the IR parts geometrically. As a result we have the gauge force and the up-down quark force with the UV and the IR parts in the molecular dynamics evolution. The reduction of the simulation cost is achieved by applying the multiple time scale integrator[22] to these three forces. We find that the relative magnitude of the force terms is given as follows:

$$\|F_G\| : \|F_{UV}\| : \|F_{IR}\| \approx 16 : 4 : 1, \quad (2.1)$$

where F_G denotes the gauge part and $F_{UV,IR}$ for the UV and the IR parts of the up-down quark. The associated step sizes $\delta\tau_G, \delta\tau_{UV}, \delta\tau_{IR}$ are chosen such that

$$\delta\tau_G \|F_G\| \approx \delta\tau_{UV} \|F_{UV}\| \approx \delta\tau_{IR} \|F_{IR}\|. \quad (2.2)$$

These step sizes are controlled by three integers N_0, N_1, N_2 as $\delta\tau_G = \tau/N_0N_1N_2, \delta\tau_{UV} = \tau/N_1N_2, \delta\tau_{IR} = \tau/N_2$ with τ the trajectory length. We fix $N_0 = N_1 = 4$ in our all simulations. The value of N_2 is adjusted to make the simulation stable. The threshold for the replay trick is chosen to be $dH = 2$.

Table 1: Summary of simulation parameters. Quark masses are perturbatively renormalized in the $\overline{\text{MS}}$ scheme at the scale of $\mu = 1/a$. The replay trick is applied for the case of $dH > 2$. MD time is the number of trajectories multiplied by the trajectory length τ . CPU time for unit τ is measured on 256 nodes of the PACS-CS computer.

κ_{ud}	0.13700	0.13727	0.13754	0.13754	0.13770	0.13781	0.137785
κ_{s}	0.13640	0.13640	0.13640	0.13660	0.13640	0.13640	0.13660
HMC	DD	DD	DD	DD	DD	MP	MP2
τ	0.5	0.5	0.5	0.5	0.25	0.25	0.25
$(N_0, N_1, N_2, N_3, N_4)$	(4,4,10)	(4,4,14)	(4,4,20)	(4,4,28)	(4,4,16)	(4,4,4,6) (4,4,6,6)	(4,4,2,4,4)
ρ_1	—	—	—	—	—	0.9995	0.9995
ρ_2	—	—	—	—	—	—	0.9990
N_{poly}	180	180	180	220	180	200	220
replay trick	on	on	on	on	on	off	off
rate of $dH > 2$	0%	0.08%	0.5%	0.1%	3%	2.8%	0.9%
MD time	2000	2000	2250	2000	2000	990	950
CPU time [hrs]	0.29	0.44	1.3	1.1	2.7	7.1	6.0
$m_{\text{ud}}^{\overline{\text{MS}}} [\text{MeV}]$	66.8(7)	45.3(5)	24.0(3)	21.0(3)	12.3(2)	3.5(2)	3.5(1)
$m_{\pi} [\text{MeV}]$	702(7)	570(6)	411(4)	385(4)	296(3)	156(2)	164(4)

For the strange quark we employ the UVPHMC algorithm, where the domain-decomposition is not used. The polynomial order N_{poly} for the UVPHMC algorithm is adjusted to keep high acceptance rate for the global Metropolis test at the end of each trajectory. Based on our observation of $\|F_{\text{s}}\| \approx \|F_{\text{IR}}\|$ for the strange quark force, we set $\delta\tau_{\text{s}} = \delta\tau_{\text{IR}}$. Calculation of the IR force requires the inversion of the Wilson-Dirac operator on the full lattice, which is carried out by the SAP (Schwarz alternative procedure) preconditioned GCR algorithm. We use the SSOR preconditioned GCR algorithm for the UV part. These preconditionings are accelerated with the single precision arithmetic. We employ the stopping condition $|Dx - b|/|b| < 10^{-9}$ for the force calculation and 10^{-14} for the Hamiltonian, which guarantees the reversibility of the molecular dynamics trajectories to high precision. The DDHMC algorithm for the up-down quark works efficiently for $\kappa_{\text{ud}} \leq 0.13770$.

As we reduce the up-down quark mass, the increasing fluctuations of the $\|F_{\text{IR}}\|$ make the simulation unstable. To suppress the fluctuations of $\|F_{\text{IR}}\|$, we incorporate the mass preconditioning for the IR part (MPDDHMC), which splits the IR force F_{IR} into F'_{IR} and \tilde{F}_{IR} by introducing a new hopping parameter $\kappa'_{\text{ud}} = \rho_1 \kappa_{\text{ud}}$ with ρ_1 less than unity. In the MPDDHMC algorithm we need four integers (N_0, N_1, N_2, N_3) to control the four step sizes $\delta\tau_{\text{G}}, \delta\tau_{\text{UV}}, \delta\tau'_{\text{IR}}, \delta\tilde{\tau}_{\text{IR}}$. N_2, N_3 and ρ_1 are adjusted to reduce the fluctuations of $\|F'_{\text{IR}}\|$ and $\|\tilde{F}_{\text{IR}}\|$. We choose $\delta\tau_{\text{s}} = \delta\tau'_{\text{IR}}$ for the strange quark force in the UVPHMC algorithm.

For the run at $\kappa_{\text{ud}} = 0.137785$ further mass preconditioning is applied to the shifted IR force F'_{IR} , which is divided into F''_{IR} and \tilde{F}'_{IR} using an additional hopping parameter $\kappa''_{\text{ud}} = \rho_2 \kappa'_{\text{ud}} = \rho_2 \rho_1 \kappa_{\text{ud}}$ with ρ_2 less than unity. We refer to this algorithm as MP2DDHMC because of two-level of mass

preconditioning. In this case five step sizes $\delta\tau_G, \delta\tau_{UV}, \delta\tau'_{IR}, \delta\tilde{\tau}'_{IR}, \delta\tilde{\tau}_{IR}$ are controlled by five integers $(N_0, N_1, N_2, N_3, N_4)$. We adjust the values of N_2, N_3, N_4 and ρ_1, ρ_2 to keep stable the fluctuations of $\|F''_{IR}\|, \|\tilde{F}'_{IR}\|, \|\tilde{F}_{IR}\|$. $\delta\tau_s$ is equal to $\delta\tau''_{IR}$.

For the MPDDHMC and the MP2DDHMC algorithms the inversion of the Wilson-Dirac operator on the full lattice is composed of three steps. Firstly, we prepare the initial solutions employing the chronological guess with the last 16 solutions. Secondly, we apply a nested BiCGStab solver consisting of the outer solver and the inner one. The latter with single precision arithmetic works as a preconditioner for the former operated with double precision. We employ a stringent stopping condition $|Dx - b|/|b| < 10^{-14}$ for the outer solver and an automatic tolerance control ranging from 10^{-3} to 10^{-6} for the inner solver. Thirdly, the nested BiCGStab solver is replaced by the GCRO-DR (Generalized Conjugate Residual with implicit inner Orthogonalization and Deflated Restarting) algorithm, once the inner BiCGStab solver becomes stagnant during the inversion of the Wilson-Dirac operator.

In Figs. 1 and 2 we show the dH and the force histories at $\kappa_{ud} = 0.13727$ and 0.13770 with the DDHMC algorithm and those at $\kappa_{ud} = 0.13781$ with the MPDDHMC algorithm. The time histories at $\kappa_{ud} = 0.13727$ are quite stable, whereas the $\kappa_{ud} = 0.13770$ case shows the spike-like fluctuations of the IR force at a few % rate of trajectories. For the $\kappa_{ud} = 0.13781$ run we observe that the MPDDHMC algorithm succeeds in reducing the fluctuations of the IR forces F'_{IR} and \tilde{F}_{IR} .

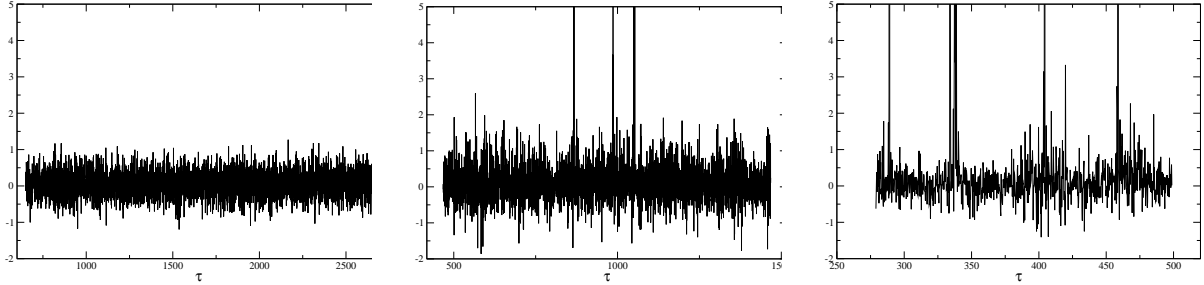


Figure 1: dH histories for $(\kappa_{ud}, \kappa_s) = (0.13727, 0.13640)$, $(0.13770, 0.13640)$ and $(0.13781, 0.13640)$ from the left.

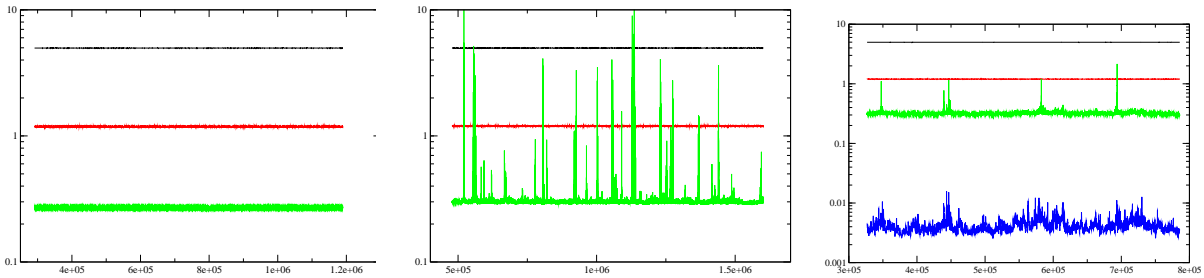


Figure 2: Force histories for $(\kappa_{ud}, \kappa_s) = (0.13727, 0.13640)$, $(0.13770, 0.13640)$ and $(0.13781, 0.13640)$ from the left. In the left and middle figures black, red and green lines denote F_G, F_{UV} and F_{IR} , respectively, with the DDHMC algorithm. In the right figure black, red, green and blue lines are for F_G, F_{UV}, F'_{IR} and \tilde{F}_{IR} , respectively, with the MPDDHMC algorithm.

3. Hadron spectrum

We measure hadron correlators at ever 10 trajectories for $\kappa_{\text{ud}} \leq 13770$ and 20 trajectories for $\kappa_{\text{ud}} \geq 13781$. Light hadron masses are extracted from single exponential χ^2 fits to the correlators with an exponentially smeared source and a local sink. In order to increase the statistics we take four source points with different time slices for $\kappa_{\text{ud}} \geq 0.13754$. They are averaged on each configuration before the jackknife analysis. This reduces the statistical errors by typically 20–40% for the vector meson and the baryon masses and less than 20% for the pseudoscalar meson masses compared to a single source point. Statistical errors are estimated by the jackknife method. Figure 3 shows the binsize dependence of the error for the pion mass and the “ η_{ss} ” meson mass. We observe that the magnitude of the error reaches a plateau after 100–200 MD time. This feature seems almost independent of the quark mass. Since similar binsize dependences are found for other particle types, we choose a binsize of 250 MD time at $\kappa_{\text{ud}} < 0.13770$. At $\kappa_{\text{ud}} = 0.13781$ we employ a binsize of 110 MD time due to the lack of statistics.

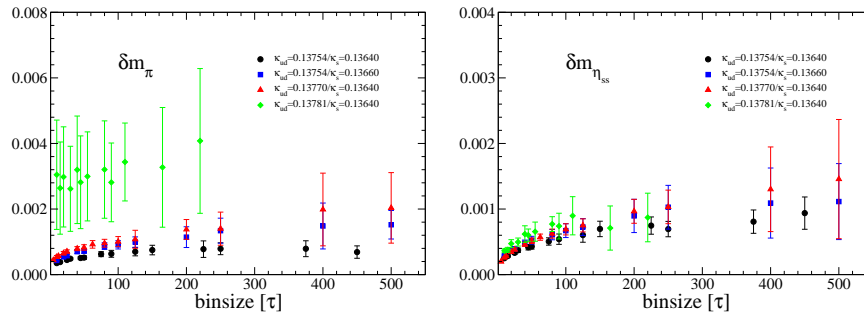


Figure 3: Binsize dependence of the magnitude of error for m_π (left) and $m_{\eta_{\text{ss}}}$ (right) at $\kappa_{\text{ud}} \geq 0.13754$

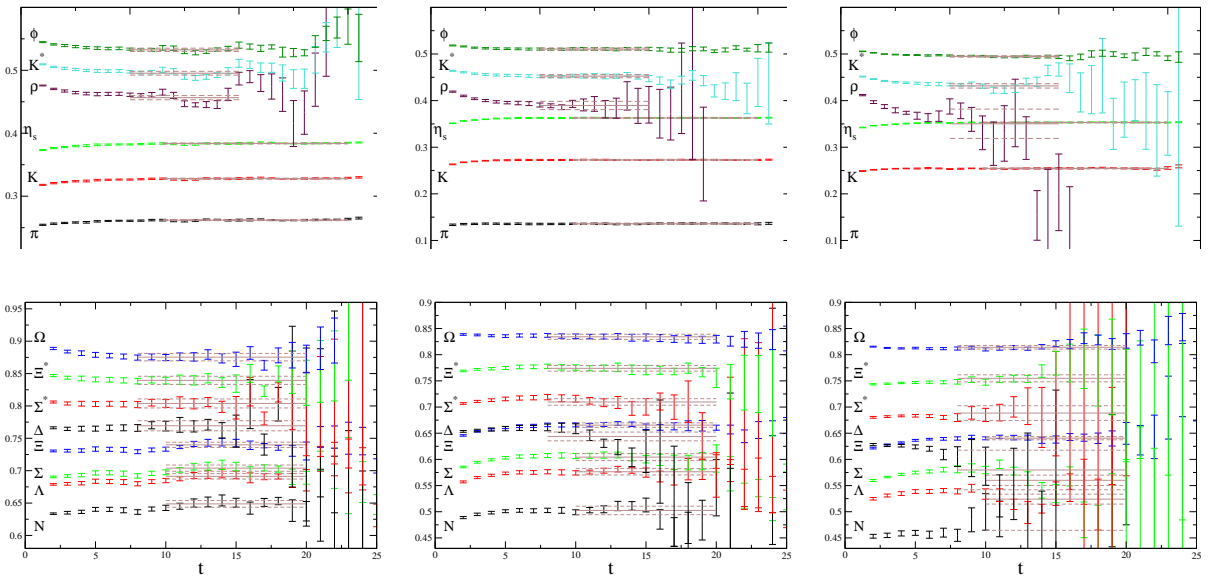


Figure 4: Effective masses for the mesons (top) and the baryons (bottom) for $(\kappa_{\text{ud}}, \kappa_s) = (0.13727, 0.13640)$, $(0.13770, 0.13640)$ and $(0.13781, 0.13640)$ from the left.

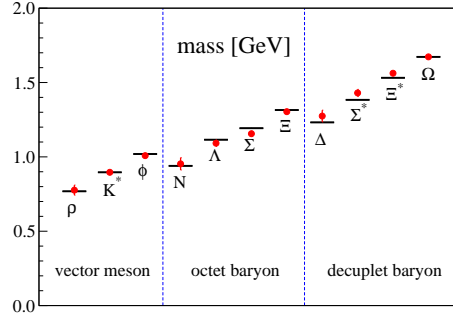


Figure 5: Light hadron spectrum extrapolated to the physical point (red circles) in comparison with the experimental values (black bars).

Figure 4 shows the hadron effective masses at $\kappa_{\text{ud}} = 0.13727, 0.13770$ and 0.13781 . We observe clear plateau for the mesons except the ρ meson at $\kappa_{\text{ud}} = 0.13781$ and also good signal for the baryons thanks to a large volume. Especially, the Ω baryon has a stable signal and a weak up-down quark mass dependence for our simulation parameters. Taking advantage of this virtue we choose the Ω baryon as input to determine the lattice cutoff. Combined with the additional inputs of m_π and m_K to determine the physical up-down and strange quark masses, we obtain $a^{-1} = 2.176(31)$ GeV. In this procedure we employ the SU(2) ChPT analyses for the quark mass dependences of m_π , m_K , f_π and f_K taking account of the finite size corrections evaluated at the one-loop level[8, 16]. For m_Ω we assume the linear quark mass dependences. With the use of this cutoff we find that the lightest pseudoscalar meson mass we have reached is about 160 MeV. To obtain the vector meson masses and the baryon masses at the physical point we avoid the chiral analyses based on the heavy meson effective theory or the heavy baryon ChPT because of their poor convergences in the chiral expansions. We instead use linear chiral extrapolations to the physical point. In Fig. 5 we compare the light hadron spectrum at the physical point with the experimental values. The largest discrepancy is at most 3%, albeit errors are still not small for the ρ meson, the nucleon and the Δ baryon. It should be also noted that our results contain possible $O((a\Lambda_{\text{QCD}})^2)$ cutoff errors.

We calculate the bare quark masses using the axial vector Ward-Takahashi identity (AWI) defined by $am^{\text{AWI}} = \lim_{t \rightarrow \infty} \langle \nabla_4 A_4^{\text{imp}}(t) P(0) \rangle / (2 \langle P(t) P(0) \rangle)$ where A_4^{imp} is the nonperturbatively $O(a)$ -improved axial vector current[23]. Employing the perturbative renormalization factors Z_A and Z_P evaluated up to one-loop level [24, 25], we obtain

$$m_{\text{ud}}^{\overline{\text{MS}}}(\mu = 2\text{GeV}) = 2.527(47)\text{MeV}, \quad m_{\text{s}}^{\overline{\text{MS}}}(\mu = 2\text{GeV}) = 72.72(78)\text{MeV}. \quad (3.1)$$

The physical up-down quark mass is 30% smaller than our lightest one $m_{\text{ud}}^{\overline{\text{MS}}}(\mu = 1/a) = 3.5$ MeV at $(\kappa_{\text{ud}}, \kappa_{\text{s}}) = (0.13781, 0.13640)$. The results for the pseudoscalar meson decay constants are given by

$$f_\pi = 134.0(4.2)\text{MeV}, \quad f_K = 159.4(3.1)\text{MeV}, \quad f_K/f_\pi = 1.189(20) \quad (3.2)$$

at the physical point with the perturbative Z_A . They are consistent with the experimental values within the errors. Our concern about the values for the quark masses and the pseudoscalar meson decay constants is the use of the perturbative renormalization factors which might cause sizable

systematic errors. We are now calculating the nonperturbative Z_A and Z_P with the Schrödinger functional scheme.

Acknowledgments

Numerical calculations for the present work have been carried out on the PACS-CS computer at Center for Computational Sciences, University of Tsukuba. A part of the code development has been carried out on Hitachi SR11000 at Information Media Center of Hiroshima University. This work is supported in part by Grants-in-Aid for Scientific Research from the Ministry of Education, Culture, Sports, Science and Technology (Nos. 16740147, 17340066, 18104005, 18540250, 18740130, 19740134, 20340047, 20540248, 20740123, 20740139).

References

- [1] PACS-CS Collaboration, S. Aoki *et al.*, PoS (LAT2005) 111.
- [2] PACS-CS Collaboration, A. Ukawa *et al.*, PoS (LAT2006) 039.
- [3] PACS-CS Collaboration, Y. Kuramashi *et al.*, PoS (LAT2006) 029.
- [4] Y. Kuramashi, PoS (LAT2007) 017.
- [5] PACS-CS Collaboration, N. Ukita *et al.*, PoS (LAT2007) 138.
- [6] PACS-CS Collaboration, D. Kadoh *et al.* PoS (LAT2007) 109.
- [7] Y. Kuramashi, these proceedings.
- [8] S. Aoki *et al.*, arXiv:0807.1661 [hep-lat].
- [9] M. Lüscher, JHEP **0305** (2003) 052; Comput. Phys. Commun. **156** (2004) 209; *ibid.* **165** (2005) 199.
- [10] A. Kennedy, Nucl. Phys. **B** (Proc. Suppl.) **140** (2005) 190.
- [11] M. Hasenbusch, Phys. Lett. **B519** (2001) 177.
- [12] M. Hasenbusch and K. Jansen, Nucl. Phys. **B659** (2003) 299.
- [13] R. Brower, T. Ivanenko, A. Levi and K. Orginos, Nucl. Phys. **B484** (1997) 353.
- [14] M. Parks *et al.*, SIAM J. Sci. Comput. **28** (2006) 1651.
- [15] PACS-CS Collaboration, K-I. Ishikawa *et al.*, PoS (LAT2006) 027.
- [16] PACS-CS Collaboration, D. Kadoh *et al.*, these proceedings.
- [17] PACS-CS Collaboration, Y. Namekawa *et al.*, these proceedings.
- [18] CP-PACS and JLQCD Collaborations, S. Aoki *et al.*, Phys. Rev. **D73** (2006) 034501.
- [19] Y. Iwasaki, preprint, UTHEP-118 (Dec. 1983), unpublished.
- [20] CP-PACS and JLQCD Collaborations, T. Ishikawa *et al.*, PoS (LAT2006) 181.
- [21] CP-PACS and JLQCD Collaborations, T. Ishikawa *et al.*, hep-lat/0704.193.
- [22] J. C. Sexton and D. H. Weingarten, Nucl. Phys. **B380** (1992) 665.
- [23] CP-PACS/JLQCD and ALPHA Collaborations, T. Kaneko *et al.*, JHEP **0704** (2007) 092.
- [24] S. Aoki *et al.*, Phys. Rev. **D58**, (1998) 074505.
- [25] Y. Taniguchi and A. Ukawa, Phys. Rev. **D58** 114503 (1998).